J. Fluid Mech. (2015), *vol.* 785, *pp.* 270–282.
doi:10.1017/jfm.2015.638

Has the ultimate state of turbulent thermal convection been observed?

L. Skrbek[1,†] and P. Urban[2]

[1]Faculty of Mathematics and Physics, Charles University, Ke Karlovu 3, 121 16 Prague, Czech Republic

[2]Institute of Scientific Instruments ASCR, v.v.i., Královopolská 147, 612 00 Brno, Czech Republic

(Received 3 July 2015; revised 10 September 2015; accepted 25 October 2015;
first published online 17 November 2015)

An important question in turbulent Rayleigh–Bénard convection is the scaling of the Nusselt number with the Rayleigh number in the so-called ultimate state, corresponding to asymptotically high Rayleigh numbers. A related but separate question is whether the measurements support the so-called Kraichnan law, according to which the Nusselt number varies as the square root of the Rayleigh number (modulo a logarithmic factor). Although there have been claims that the Kraichnan regime has been observed in laboratory experiments with low aspect ratios, the totality of existing experimental results presents a conflicting picture in the high-Rayleigh-number regime. We analyse the experimental data to show that the claims on the ultimate state leave open an important consideration relating to non-Oberbeck–Boussinesq effects. Thus, the nature of scaling in the ultimate state of Rayleigh–Bénard convection remains open.

Key words: turbulent convection, turbulent flows

1. Introduction

Although the equations describing turbulent buoyancy driven flows and the corresponding convective heat transfer have been known for a long time (Tritton 1988), our ability to predict the intense convection occurring at large scales in the atmosphere, ocean, stars or Sun is very limited or non-existent. This is true even for the simplest model flow – the ideal laterally infinite Rayleigh–Bénard convection occurring in an Oberbeck–Boussinesq fluid layer confined between two perfectly conducting plates; the bottom plate is heated and the top plate is cooled. Rayleigh–Bénard convection is fully characterized by the Rayleigh number, $Ra = g(\alpha/\nu\kappa)\Delta TL^3$, and the Prandtl number, $Pr = \nu/\kappa$. Here, g is the acceleration due to gravity, α is the isobaric thermal expansion coefficient of the fluid, ν and κ are the fluid viscosity and thermal diffusivity respectively, $\Delta T = T_b - T_t$ is the difference between the top and bottom wall temperatures, denoted by suffixes t and b respectively, and L is the vertical separation between the top and bottom walls. The combination $\eta = \alpha/(\nu\kappa)$ is often a useful combination. Organized features such as plumes, jets and large-scale circulation, known as 'wind' (Niemela *et al.* 2001), of the mean velocity U, with a size comparable to the size of the convective layer, L, are known to exist in the flow and can be characterized by the flow Reynolds number, $Re = UL/\nu$.

† Email address for correspondence: skrbek@nbox.troja.mff.cuni.cz

The ability of the convective motion to transfer heat from the heated bottom plate to the cooled top plate, i.e. the convective heat transfer effectiveness, is described by the Nusselt number, $Nu = L\dot{q}/\lambda\Delta T$, via the $Nu = Nu(Ra; Pr)$ dependence. Here, $\dot{q}$ is the total convective heat flux density and λ denotes the thermal conductivity of the fluid. The relation $Nu = Nu(Ra; Pr)$ is usually expressed in the form of a dimensionless scaling law $Nu \propto Ra^{\gamma} Pr^{\beta}$. A number of theoretical models have been developed (see Ahlers, Grossmann & Lohse (2009), Chillà & Schumacher (2012) and original references therein). We should explicitly mention that two independent theories of Castaing *et al.* (1989) and Shraiman & Siggia (1990) predict $\gamma = 2/7$, while Malkus (1954) and Priestley (1959) derived $\gamma = 1/3$ in a model where heat transfer is controlled by the heat conduction of marginally stable boundary layers which become thinner with increasing heat flux; in their model, the heat transport does not depend on the height L and all of the temperature difference ΔT occurs within the boundary layers which are thin in comparison with L, while the central turbulent fluid is effectively mixed and has a constant temperature $T_m = (T_t + T_b)/2$.

At very high Ra, Rayleigh–Bénard convection is thought to enter the so-called ultimate, or asymptotic, regime, although it is not known with any certainty the Rayleigh numbers above which this state sets in. Kraichnan (1962) postulated that the heat transport mechanisms in this regime become independent of ν and κ, because the boundary layers would be turbulent and fully developed. The phenomenologically predicted scaling law, for $0.15 < Pr < 1$, is of the form $Nu \propto Ra^{1/2} Pr^{-1/4} (\log Ra)^{-3/2}$; for the conjecture on the ultimate $Nu \propto (PrRa)^{1/2}$, see also Spiegel (1971). An alternative theoretical model has been proposed by Grossmann & Lohse (2000) and recently updated by Stevens *et al.* (2013) but, since this model does not have absolute predictive power concerning the transition to the ultimate regime, we shall not consider it any further. One has to consider that when developing the model Kraichnan used what was known about turbulent boundary layers at that time; however, much more has been learnt about them since 1962. There is a clear call to theorists to repeat Kraichnan's calculations as diligently as he did, but with the modern outlook on boundary layers and turbulent convection itself, until then, one should not take his prediction seriously on its own. Rigorous theory regards the problem of $Nu(Ra, Pr)$ scaling at very high Ra (even in the simplest case of laterally infinite Rayleigh–Bénard convection) as open (Doering 2012), in the sense that rigorous analysis does not preclude it, but, at the same time, does not prove that any flow can possibly realize it. This issue seems unlikely to be resolved numerically in the near future (Ahlers *et al.* 2009; Chillà & Schumacher 2012), therefore experimental investigations under controlled laboratory conditions are crucial.

In applications, it is hard to overestimate the importance of this asymptotic regime for deeper understanding of a number of natural phenomena (Ahlers *et al.* 2009). Typical values of Ra for convection in the atmosphere, ocean or Sun are extremely high (Sreenivasan 1998), and extrapolation of the heat transport efficiency from the presently known experimental or computational data may lead to uncertainties of up to an order of magnitude, due to uncertainties in γ. A convenient identification of the transition to the ultimate regime is made when, upon increasing Ra, the scaling exponent γ starts to exceed the value of $1/3$. We emphasize, however, that our considerations so far have assumed an Oberbeck–Boussinesq working fluid of constant physical properties except for its density which linearly depends on temperature. However, this is never exactly valid in practice and, as we shall see, causes severe problems in experiments reaching very high Ra.

Observation of the transition to the ultimate state of Rayleigh–Bénard convection has been claimed several times – in the Grenoble cryogenic helium experiments

(Chavanne *et al.* 1997, 2001; Roche *et al.* 2010) and in the SF_6 Göttingen experiments at ambient temperature (Ahlers *et al.* 2012*b*; He *et al.* 2012*a*,*b*, 2014). This paper extends our recent experimental studies considerably (Urban, Musilová & Skrbek 2011; Urban *et al.* 2012, 2014), where we discussed in detail issues such as the influence of the shape (aspect ratio) and material properties of the experimental cells, various corrections to the raw data and advantages of using a clean cryogenic environment. Here, we do not discuss details of experimental corrections applied to the experimentally measured raw data; rather, we concern ourselves exclusively with the non-Oberbeck–Boussinesq effects. The following detailed analysis shows that the claims of observing transition to the ultimate state of Rayleigh–Bénard convection could indeed be related to non-Oberbeck–Boussinesq effects.

2. The experimental cells

We start with a brief description of the experimental cells in which it is claimed that the transition to the ultimate state has been observed.

The Grenoble cells. The first claim of observing the transition (described as 'possibly corresponding to the asymptotic regime predicted by R. Kraichnan') by Chavanne *et al.* (1997) – see also Chavanne *et al.* (2001) – results from a cylindrical aspect ratio $\Gamma = 1/2$ cell 20 cm in height. Similar results, displaying the transition to what was later called the 'Grenoble regime', have been observed in seven cryogenic convection cells, differing in various details, see figures 2 and 3 of Roche *et al.* (2010). All of them are cylindrical, of diameter $D = 10$ cm and height, L, of 8.8 cm (Short cell), 43 cm (Cigar cell) and 20 cm (Flange, Paper, Screen, Vintage and ThickWall, i.e. all remaining ones), corresponding respectively to aspect ratios of $\Gamma = 1.14$, 0.23 and 0.50.

Although the transition to the ultimate, or Grenoble, state has been observed in all of these cells, we find it useful to divide them into three groups, simply by their absolute height, L. The common feature of cells with $L = 20$ cm is that they all displayed the local scaling exponent characterizing the heat transport efficiency via $Nu = Nu(Ra)$, crossing the value of $1/3$ at approximately 10^{11}–10^{12} in Ra. The Short cell displays this same feature but at significantly lower Ra. Finally, the scaling exponent measured in the Cigar cell displays an almost constant value of approximately $1/3$ until Ra reaches approximately 5×10^{12}, where it steeply rises. It should be noted that, if Ra were rescaled assuming the same height (20 cm) for all of the Grenoble cells (i.e. a factor of eight up for the Short cell and the same factor down for the Cigar cell), the observed transitions to the Grenoble state would almost collapse if Nu were plotted versus this rescaled Ra. Let us emphasize that in Grenoble cells the transitions have been observed several times under strictly fixed values of Pr (Roche *et al.* 2010), i.e. the possible $Nu(Pr)$ dependence cannot be identified as a reason for the observed transition.

The Göttingen cells. Transitions to the ultimate state has been claimed (at $Pr \lesssim 1$) in three cylindrical cells of diameter $D = 1.12$ m: $\Gamma = 1/2$ (i.e. $L = 2.24$ m) (Ahlers *et al.* 2012*b*; He *et al.* 2012*b*), $\Gamma = 1$ (He *et al.* 2012*a*) and, most recently, $\Gamma = 1/3$ (He *et al.* 2014). All of these cells were located in the 'Uboot of Göttingen', a pressure vessel of approximately 25 m^3 volume able to contain up to 2000 kg of the working fluid (SF_6) at pressures of up to 19 bars. The sidewall insulated by thermal shields was made of 9.5 mm thick Plexiglas sealed to aluminium top and bottom plates. For most recent experiments cited here (after the authors dealt with the 'chimney effect', by sealing the originally existing gap between the plates and the sidewall), at the mid-height of the sidewall, there was a hole connected to a remotely controlled valve,

via a tube of 13 mm inner diameter. Before each measurement sequence, the valve was opened and the sample cell and Uboot were filled with (SF_6) to the desired pressure. Then, after all pressure and temperature transients had decayed, the valve was closed and the desired measurements were made on a completely closed sample.

We now consider complementary experimental cells reaching very high Ra but displaying no transition to the ultimate state.

The Chicago, Oregon/Trieste and Brno cells have been used in clean cryogenic conditions with cryogenic He gas as working fluid. The largest Chicago cell used in the experiments of Wu (1991) – see also Castaing *et al.* (1989) – was identical in shape to the Chavanne cell (Chavanne *et al.* 1997; Roche *et al.* 2010) but twice as large ($L = 40$ cm); values of Ra of up to 2×10^{14} were obtained.

The original Oregon/Trieste cell (Niemela *et al.* 2000), of the same shape as above, is the largest ($L = 100$ cm) cryogenic cell used so far. No sign of transition was observed up to so far the highest $Ra \approx 10^{17}$. The least-square fit of the Nusselt number versus Rayleigh number for the original 'Oregon' data spanning 11 orders of Ra in turbulent convection up to 10^{17} yields a $\mathrm{d}\log Nu/\mathrm{d}\log Ra$ slope of 0.32 (Niemela & Sreenivasan 2006). The design of the Oregon cell is close to the Flange Grenoble cell (Roche *et al.* 2010) – its sidewall consists of two equal halves, allowing a simple change to the $\Gamma = 1$ cell ($L = 50$ cm), which was later used in Trieste (Niemela & Sreenivasan 2003, 2006, 2010).

Our cylindrical $\Gamma = 1$ Brno cell (Urban *et al.* 2010) is slightly smaller ($L =$ 30 cm), capable of covering the range $10^6 < Ra < 10^{15}$ with sufficient precision of measurements.

We point out here that in earlier work (Funfschilling, Bodenschatz & Ahlers 2009) the $\Gamma = 1/2$ Göttingen cell has been used to explore the global heat transport with other working fluids in addition to SF_6 ($Pr = 0.79$–0.84), namely with gaseous He ($Pr = 0.67$) and N_2 ($Pr = 0.72$) at near-ambient temperatures, altogether covering the $10^9 \lesssim Ra \lesssim 3 \times 10^{14}$ range. These measurements did not reveal any sign of the transition to the ultimate regime and were claimed to be roughly consistent with the cryogenic Oregon data but inconsistent with the Grenoble results.

3. Analysis

In our previous study (Urban *et al.* 2011), we have shown that for $7.2 \times 10^6 \leqslant Ra \leqslant 10^{11}$ our sidewall-corrected data agree with suitably corrected data from complementary cryogenic experiments, and are consistent with $Nu \propto Ra^{2/7}$. On approaching $Ra \approx 10^{11}$, all cryogenic data display a broad crossover to $Nu \propto Ra^{1/3}$, as predicted by the theory (Malkus 1954; Priestley 1959). It is mainly above approximately 10^{12} in Ra that strong differences appear.

Here, we show that the probable reason for this disagreement is a gradual departure from the Oberbeck–Boussinesq conditions upon increasing Ra in each particular cell. To justify that the fluid sample can be treated as Oberbeck–Boussinesq in high-Ra experiments, various phenomenological requirements have usually been applied, such as $\alpha(T_b - T_t) < C$, with C typically up to 0.2 (Niemela & Sreenivasan 2003). As a result of our experimental study, based on figure 3 in Urban *et al.* (2012) we concluded, however, that it is hard to set any simple quantitative criterion justifying the validity of Oberbeck–Boussinesq conditions.

The gradual departure from the Oberbeck–Boussinesq conditions with increasing Ra gives rise to asymmetry between the boundary layers on the top and bottom plates. We illustrate this feature in figure 1 for the $\Gamma = 1$ (He *et al.* 2012*a*) and $\Gamma = 1/2$

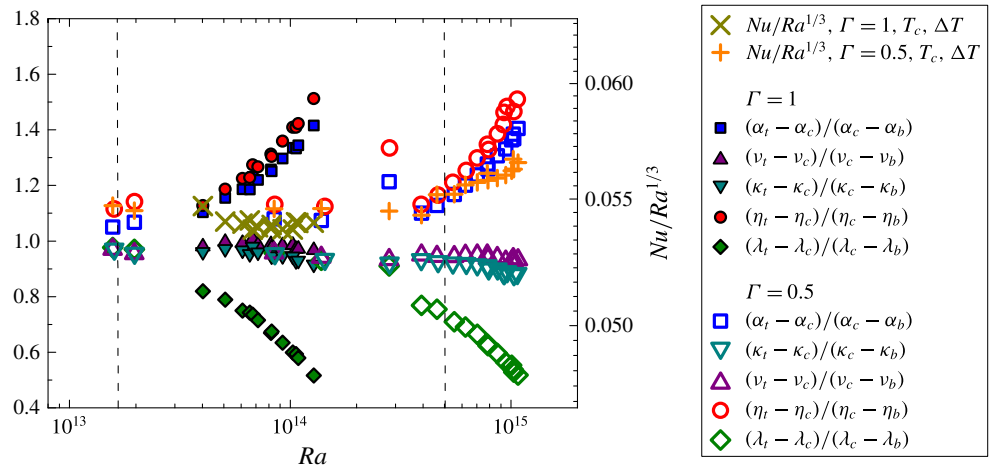

FIGURE 1. (Colour online) Growing asymmetry with increasing Ra of relative changes in relevant fluid properties for the Göttingen $\Gamma = 1$ (He *et al.* 2012*a*) and $\Gamma = 1/2$ (He *et al.* 2012*b*) experiments. Plots of dimensionless combinations of the physical quantities α, ν, κ, $\eta = \alpha/(\nu\kappa)$ and λ as indicated in the legend (left axis) evaluated at T_t, T_b and T_c versus Ra_c (for these Göttingen data sets, the result hardly changes if T_m is used instead of T_c) are shown to be closely correlated with the increase in the local power law exponent γ in the observed $Nu = Nu(Ra)$ scaling, plotted here in the compensated form as $Nu/Ra^{1/3}$ (right axis). The vertical dashed lines indicate where the transition to the ultimate state was claimed by He *et al.* (2012*b*).

(He *et al.* 2012*b*) Göttingen experiments, making use of the known SF_6 properties. (To evaluate the SF_6 properties we use the same computer program as the Göttingen group, kindly provided to us by G. Ahlers and X. He.) The results of this analysis for other cells mentioned in the previous section look similar. For an additional example of the influence of the non-Oberbeck–Boussinesq conditions on the effectiveness of heat transport, plotted in a different way for our own cryogenic He data, see figure 6 of Urban *et al.* (2014).

In order to quantify the effect of boundary layer asymmetry on the heat transfer efficiency, we follow Wu & Libchaber (1991) and use their X parameter, defined as $X = (T_c - T_t)/(T_b - T_c)$. Where available, we use the experimentally measured temperature T_c of the (almost isothermal) cell interior and evaluate $X = X_{expt}$. Whenever T_c is not available, we use the following simple idea to estimate $X = X_{th}$. The underlying physics of Malkus' theory is such that the temperature drop occurs entirely across the two boundary layers, the fluid in the bulk of the apparatus being almost isothermal. The boundary layers, of thicknesses d_b and d_t, are assumed to be marginally stable, meaning that the bottom and top Rayleigh numbers Ra_{BL}^{crit}, calculated on the basis of the boundary layer thicknesses d_b, d_t and characteristic fluid properties $[\alpha/(\nu\kappa)]_b$ and $[\alpha/(\nu\kappa)]_t$, are equal. We therefore write

$$g\left(\frac{\alpha}{\nu\kappa}\right)_b d_b^3(T_b - T_c) = g\left(\frac{\alpha}{\nu\kappa}\right)_t d_t^3(T_c - T_t) = Ra_{BL}^{crit}. \tag{3.1}$$

The heat flux $\dot{q}$ passes both (laminar) boundary layers, and assuming that Fourier's law holds, we can infer

$$\dot{q} \propto \frac{\lambda_b}{d_b}(T_b - T_c) = \frac{\lambda_T}{d_T}(T_c - T_t), \tag{3.2}$$

where we introduced the characteristic thermal conductivities of the boundary layers. This allows us to replace the ratio d_b/d_t with the combination $(\lambda_B/\lambda_T)/X$ and estimate the X parameter as

$$X = X_{th} = \frac{T_c - T_t}{T_b - T_c} = \left[\frac{\left(\dfrac{\alpha}{\nu\kappa}\right)_b}{\left(\dfrac{\alpha}{\nu\kappa}\right)_t} \left(\frac{\lambda_b}{\lambda_t}\right)^3 \right]^{1/4}. \tag{3.3}$$

The characteristic bottom (top) boundary layer properties can be estimated as arithmetic means of fluid properties evaluated at T_m and T_b (T_t); these are available for all cryogenic as well as Göttingen experiments. Figure 2 plots the X parameter evaluated by us for a number of experimental cells using (3.3) as well as, where available, based on the direct measurements of T_c. It has to be emphasized that the X parameter is not an analytical function of Ra; it depends on the size (and generally on the shape) of the convection cell and on the choice of the working point on the p–T phase diagram. For high-Rayleigh-number experiments of the Rayleigh–Bénard type, however, the X parameter serves as a useful measure of how closely the Oberbeck–Boussinesq conditions are satisfied, provided that both T_t and T_b lie on the same side of the saturated vapour pressure (SVP) curve or critical isochore in the pressure/temperature (p, T) phase diagram of the working fluid used in the particular experiment.

Given the crudeness of our model, one cannot expect exact quantitative agreement between values of the experimentally deduced $X = X_{expt}$ parameter and those predicted by (3.3) ($X = X_{th}$). Figure 2 shows, however, fairly good agreement in behaviour, both quantities departing down from unity with increasing Ra.

As T_c was not directly measured in the Grenoble cryogenic experiments (Chavanne *et al.* 1997; Roche *et al.* 2010), we rely on this similarity (and on Occam's razor reasoning) in drawing the following conclusion: for experimental reasons (size of the cell, choice of the working point), the Grenoble claims of observing the transition to the ultimate/Grenoble regime of Rayleigh–Bénard convection are most likely not justified, as the transition values of Ra were reached when the X parameter strongly suggested non-Oberbeck–Boussinesq conditions. Moreover, there are complementary experiments with the X value nearly unity, both He cryogenic (Wu 1991; Niemela *et al.* 2000; Urban *et al.* 2012) and SF_6 (He *et al.* 2012*b*), covering the range of Ra (with nearly constant $Pr \lesssim 1$) where the transition is claimed in the Grenoble experiments, and they show no sign of the transition, at least up to 10^{13} in Ra. (An additional supporting argument is that suppression of the large-scale flow, by inserting planar obstacles in the Grenoble $\Gamma = 1/2$ Screen cell of 20 cm in height, hardly affected the observed heat transfer efficiency (Roche *et al.* 2010). This is a surprising result, as the large-scale flow, sweeping the fluid across plates, is assumed to stimulate the laminar to turbulent transition of boundary layers.)

Here, we have to repeat the warning already expressed in Urban *et al.* (2014). The high-Ra ranges of the Trieste and Grenoble experiments have often been investigated using a working point (p, T_m) in the ^{4}He phase diagram close to the critical isochore. For small ΔT, our analysis is not applicable, as both boundary layers will be affected and the above assumption that one of the boundary layers can be treated as Oberbeck–Boussinesq is not justified. Moreover, on the basis of the analysis of Ahlers *et al.* (2007) of the non-Oberbeck–Boussinesq effects in gaseous ethane, one may expect that the asymmetry of the boundary layers might be partly cancelled if T_b and T_t lie on opposite sides of the critical isochore in the (p, T) phase diagram. Further experiments are needed to clarify this issue.

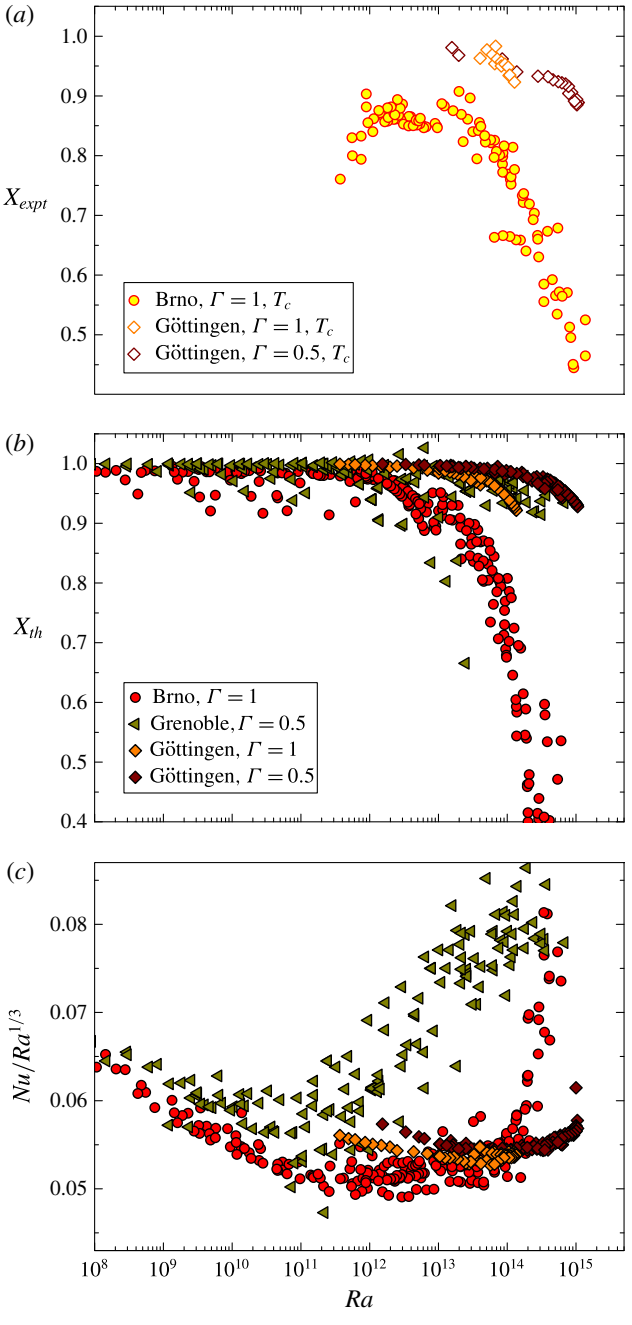

FIGURE 2. (Colour online) The asymmetry X parameter plotted versus Ra for various experiments as indicated. We plot both its experimental values, $X = X_{expt}$, based on the direct measurements of T_c (where available, (*a*)) as well as its theoretically estimated value, $X = X_{th}$, (3.3) (*b*). Panel (*c*) (the meaning of the symbols is as in (*b*)) shows the observed $Nu(Ra)$ scaling for experiments, with Nu and Ra appropriately corrected, calculated in a conventional way, i.e. based on $\Delta T = T_b - T_t$ and fluid properties evaluated at $T_m = (T_t + T_b)/2$.

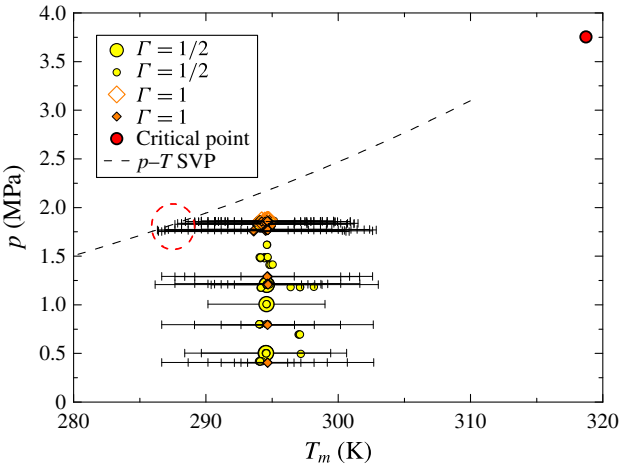

FIGURE 3. (Colour online) The p–T phase diagram of SF_6, showing the working points used in the Göttingen experiments.

Our analysis assumes that there are not multiple steady stages of high-Ra convective flow, such as those that have been recently observed in turbulent von Karman flows – for details see Thalabard *et al.* (2015) and references therein.

Let us now examine the Göttingen SF_6 data. Figure 3 shows where in the p–T phase diagram the $\Gamma = 1/2$ (He *et al.* 2012*b*) and $\Gamma = 1$ (He *et al.* 2012*a*) SF_6 data lie. We see that T_m was kept roughly constant (except for four data points that are not significant for the following discussion); higher values of Ra were obtained by increasing the pressure (vertically, towards the dashed SVP line) and then by increasing ΔT. The horizontal 'error bars' show the span of the internal cell temperature for each particular data point – their left (right) ends correspond to T_t (T_b). The critical point (red symbol) far away does not play any significant role here; however, we see that in some cases (encircled) the T_t values are dangerously close to the SVP line (representing the equilibrium first-order liquid–gas phase transition where due to fluctuations condensation/evaporation could take place), and these are precisely those data points that display the reputed $Nu = Nu(Ra)$ transition to the ultimate state! We can further strengthen our argument by pointing out the work of Zhong, Funfschilling & Ahlers (2009), showing that the heat transfer efficiency would be considerably enhanced if condensation/evaporation processes were to take place in the vicinity of the SVP line at the top plate of the SF_6 cell.

Upon increasing Ra, the top half of the cell becomes affected by the non-Oberbeck–Boussinesq effects, while the bottom half, if lying sufficiently far away from the SVP curve, does not. This scenario is confirmed by the X parameter behaviour as discussed above, see figure 2. In this situation, we can apply the approach that we just described in detail to our own He cryogenic data (Urban *et al.* 2014). In short, one can avoid the non-Oberbeck–Boussinesq effects in the top half of the cell, by replacing it with the inverted (with respect to T_c) nearly Oberbeck–Boussinesq bottom half, thus eliminating the boundary layer asymmetry. (It should be noted that for $X = 1$ (fully Oberbeck–Boussinesq case), such an operation does not change the observed $Nu = Nu(Ra)$ scaling.) This leads to effective values $\Delta T_{eff} = 2(T_b - T_c)$, Nu_{eff} and Ra_{eff} (evaluated at T_c), changing both Nu and Ra. It is important to emphasize that not only the Nusselt number scaling, but the scaling of any other independently measured

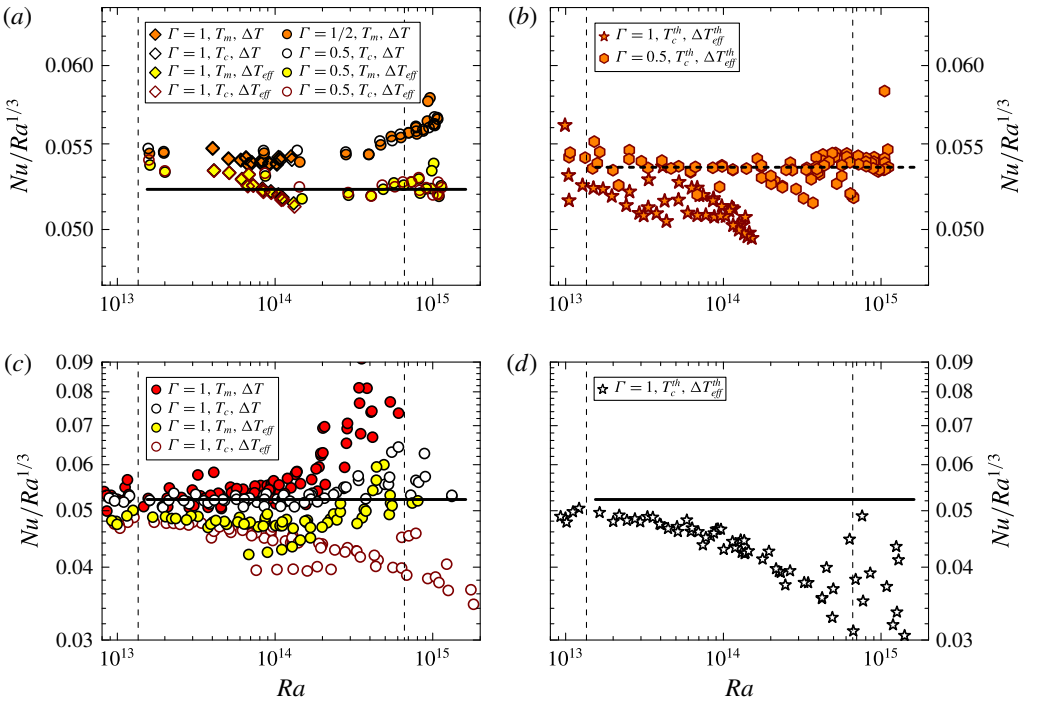

FIGURE 4. (Colour online) (*a*,*c*) The $Nu/Ra^{1/3}$ versus Ra plots of the Göttingen data (He *et al.* 2012*a*,*b*) (*a*) and the Brno cryogenic He data (Urban *et al.* 2014) (*c*); Nu and Ra are calculated based on the SF_6 and He properties at T_m, T_c, ΔT and ΔT_{eff} as indicated. The vertical dashed lines indicate where the transition to the ultimate state was claimed (He *et al.* 2012*b*). (*b*,*d*) The same Nu and Ra Göttingen data (*b*) and Brno cryogenic He data (*d*), but calculated using the experimentally measured and tabulated T_b and T_t only, with $\Delta T_{eff}^{th} = (T_b - T_c^{th})$, where T_c^{th} is evaluated for all available experimental data points using the theoretically estimated value X_{th}, (3.3). It should be noted that for the SF_6 experiments there are more data points in (*b*). The reason is that this approach does not require experimental values of T_c (which for (*a*) we calculated using Ahlers *et al.* (2012*a*)), and we used all T_b, T_t data points tabulated in Ahlers *et al.* (2012*b*). The theoretically estimated $Nu = Nu(Ra)$ scalings, for both the nearly constant Pr SF_6 Göttingen data (He *et al.* 2012*a*,*b*) (*a*,*b*) and the Brno cryogenic He data where Pr increases at the high-Ra end (Urban *et al.* 2014) (*c*,*d*), indicate no transition to the ultimate state.

quantity, such as the Reynolds number $Re = Re(Ra)$, that might have displayed 'phase transitions' spuriously interpreted as independent confirmation of the transition to the ultimate regime, will change, as well.

We have already applied this approach to our He experiments (Urban *et al.* 2014), where, however, Pr changes at the high end of attainable Ra, which complicates any definite conclusion of a possible transition to the ultimate state, see figure 4(*c*). Figure 4(*a*) displays the nearly constant Pr SF_6 original data of He *et al.* (2012*a*,*b*) together with those re-evaluated by us using the data of Ahlers *et al.* (2012*a*) in order to calculate T_c, which is then used to evaluate both $\Delta T_{eff} = 2(T_b - T_c)$ and the relevant fluid properties. We see (yellow-filled large symbols) that the $Nu_{eff} \propto Ra_{eff}^{1/3}$ scaling is closely followed.

It is interesting to examine the influence of the difference in $Nu = Nu(Ra)$ scaling depending on whether the fluid properties are evaluated conventionally, at T_m, or at the directly measured T_c. We start with Ra and Nu still based on the total $\Delta T = T_b - T_t$. We have shown (Urban *et al.* 2012, 2014) that for $10^{12} \lesssim Ra \lesssim 10^{15}$, $Nu \propto Ra^{1/3}$ within the experimental error, if the properties of the working fluid – cryogenic He gas – are evaluated at T_c, while their conventional evaluation at $T_m = (T_t + T_b)/2$ lead to spuriously steeper $Nu(Ra)$ scaling, see figure 4(*c*). Indeed, as the bulk of the Rayleigh–Bénard convection cell has temperature close to T_c, we agreed with Wu & Libchaber (1991) that it is physically natural to define Ra, Nu and Pr based on fluid properties evaluated at this temperature rather than T_m. Although this question is interesting in its own right, for the reanalysis of the Göttingen SF_6 data, the particular choice of temperature – either T_m or T_c – hardly matters for evaluating fluid properties (figure 4*a*; see also He *et al.* 2013). For SF_6 they differ only marginally while for our own data (Urban *et al.* 2012, 2013) the influence turns out to be significant.

What appears to be important for both the He and SF_6 data is the difference $\Delta T = T_b - T_c$ versus $\Delta T_{eff} = 2(T_b - T_c)$. Figure 4(*c*) shows that, in the latter case, our cryogenic He data, rather than increasing local scaling exponent γ, display slightly less steep than 1/3 scaling, most likely due to a gradually increasing Pr with Ra (Urban *et al.* 2014). On the other hand, the nearly constant Pr SF_6 Göttingen data (He *et al.* 2012*a*,*b*) closely follow the 1/3 scaling, independently of whether SF_6 properties are evaluated at T_m or at T_c, see figure 4(*a*).

Another independent check that our approach is meaningful is illustrated in figure 4(*b*,*d*), where we calculated the $Nu = Nu(Ra)$ scaling for SF_6 (*b*) and cryogenic He (*d*) theoretically, using the directly measured and tabulated values of T_t and T_b and calculating $\Delta T_{eff}^{th} = (T_b - T_c^{th})$, where T_c^{th} is evaluated for all the available experimental data points using the theoretically estimated value X_{th}, (3.3). Our simple theoretical model clearly confirms that neither the SF_6 data of He *et al.* (2012*a*,*b*) nor our cryogenic He data (Urban *et al.* 2014) indicate any transition to the ultimate state, and our theoretical model prediction confirms the tendency seen in the corresponding figures 4(*a*) and 4(*c*).

For the $\Gamma = 0.33$ Göttingen cell (He *et al.* 2014), we do not have access to the raw data in order to perform a similar detailed analysis. One can predict, however, that under similar experimental conditions (i.e. choosing similar working conditions in the SF_6 phase diagram as shown in figure 3) the transition due to the non-Oberbeck–Boussinesq effects will occur at $(0.33/0.5)^3 \approx 3.4$ times higher characteristic Ra^{NOB} due to the 1.5 times taller cell. This is illustrated in figure 5, which shows the digitized data from the single figure of He *et al.* (2014), together with the same $\Gamma = 0.33$ data shifted down in Ra by a factor of $\cong 3.4$ and consequently reduced by this shifted value of Ra in power 0.312. This operation is somewhat artificial (it is exact only for 1/3 power law scaling), but it is essentially correct; the open circles cannot be treated in the same way as the experimental data obtained in the $\Gamma = 1/2$ cell, but the purpose of this operation is to show that the non-Oberbeck–Boussinesq effects (assuming similar working points in the (p, T) phase diagram) start to be significant at approximately the same Ra^{NOB}. The situation is therefore similar to the Grenoble cells discussed above. Additionally, figure 5 indicates that the highest-Ra $\Gamma = 0.33$ and $\Gamma = 1/2$ data (i.e. the data points closely following the shown lines of $Nu \propto Ra^{0.38}$ scaling (He *et al.* 2014)) nearly collapse if the former are shifted by this factor down in Ra, contrary to the expectation that transition to the ultimate regime in cells of the same diameter would take place at some universal Ra^*.

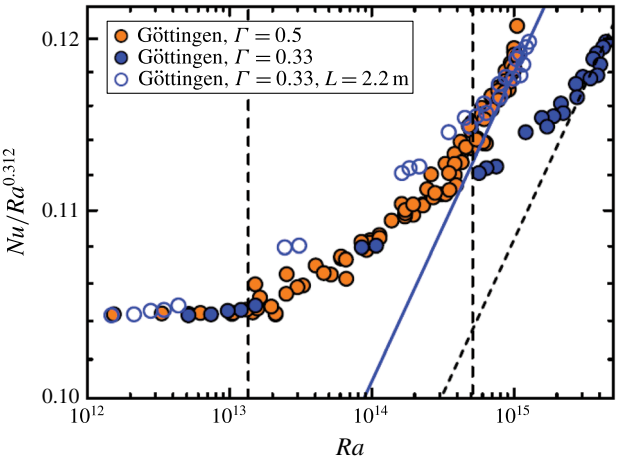

FIGURE 5. (Colour online) The $Nu/Ra^{0.312}$ versus Ra plots of the Göttingen data, digitized using figure 1 of He *et al.* (2014). Solid blue symbols represent the data obtained in the $\Gamma = 0.33$ cell, solid orange symbols represent those from the $\Gamma = 1/2$ cell of the same diameter, open blue symbols are the solid blue symbols but shifted by a factor of $(0.33/0.5)^3$ down in Ra. The black vertical dashed lines Ra_1^* (left) and Ra_2^* (right) indicate where the transition to the ultimate state was claimed (He *et al.* 2012*b*). The black dashed line represents $Nu = 0.01035Ra^{0.38}$, while the blue solid line is the same but shifted by a factor of $(0.33/0.5)^3$ down in Ra.

4. Conclusions

To conclude, we have reanalysed the data of very-high-Ra experiments, focusing on those claiming to have observed the transition to the ultimate state of Rayleigh–Bénard convection. Our analysis strongly suggests that the present claims (Chavanne *et al.* 1997, 2001; Roche *et al.* 2010; He *et al.* 2012*a*,*b*, 2014) are most likely not justified, leaving open an important consideration of relating them to non-Oberbeck–Boussinesq effects, and the very important and intriguing question of the transition (if it occurs) to the ultimate state of Rayleigh–Bénard convection remains open.

Acknowledgements

We thank P. Hanzelka, X. He, M. La Mantia and V. Musilová for stimulating discussions. The support of the Czech Science Foundation under GAČR 203/14/02005S is warmly acknowledged.

REFERENCES

AHLERS, G., ARAUJO, F. F., FUNFSCHILLING, D., GROSSMANN, S. & LOHSE, D. 2007 Non-Oberbeck–Boussinesq effects in gaseous Rayleigh–Bénard convection. *Phys. Rev. Lett.* **98**, 054501.

AHLERS, G., BODENSCHATZ, E., FUNFSCHILLING, D., GROSSMANN, S., HE, X. Z., LOHSE, D., STEVENS, R. J. A. M. & VERZICCO, R. 2012*a* Logarithmic temperature profiles in turbulent Rayleigh–Bénard convection. *Phys. Rev. Lett.* **109**, 114501.

AHLERS, G., GROSSMANN, S. & LOHSE, D. 2009 Heat transfer and large scale dynamics in turbulent Rayleigh–Bénard convection. *Rev. Mod. Phys.* **81**, 503–537.

AHLERS, G., HE, X., FUNFSCHILLING, D. & BODENSCHATZ, E. 2012*b* Heat transport by turbulent Rayleigh–Bénard convection for $Pr \simeq 0.8$ and $3 \times 10^{12} \lesssim Ra \lesssim 10^{15}$: aspect ratio $\Gamma = 0.50$. *New J. Phys.* **14**, 103012.

CASTAING, B., GUNARATNE, G., HESLOT, F., KADANOFF, L., LIBCHABER, A., THOMAE, S., WU, X. Z., ZALESKI, S. & ZANETTI, G. 1989 Scaling of hard thermal turbulence in Rayleigh–Bénard convection. *J. Fluid Mech.* **204**, 1–30.

CHAVANNE, X., CHILLÀ, F., CASTAING, B., HÉBRAL, B., CHABAUD, B. & CHAUSSY, J. 1997 Observation of the ultimate regime in Rayleigh–Bénard convection. *Phys. Rev. Lett.* **79**, 3648–3651.

CHAVANNE, X., CHILLÀ, F., CHABAUD, B., CASTAING, B. & HÉBRAL, B. 2001 Turbulent Rayleigh–Bénard convection in gaseous and liquid He. *Phys. Fluids* **13**, 1300–1320.

CHILLÀ, F. & SCHUMACHER, J. 2012 New perspectives in turbulent Rayleigh–Bénard convection. *Eur. Phys. J.* E **35**, 58.

DOERING, C. R. 2012 Rigorous results for heat transport in high Rayleigh number convection. In *International Conference on RB Turbulence, Hong Kong*.

FUNFSCHILLING, D., BODENSCHATZ, E. & AHLERS, G. 2009 Search for the 'ultimate state' in turbulent Rayleigh–Bénard convection. *Phys. Rev. Lett.* **103**, 014503.

GROSSMANN, S. & LOHSE, D. 2000 Scaling in thermal convection: a unifying theory. *J. Fluid Mech.* **407**, 27–56.

HE, X., FUNFSCHILLING, D., BODENSCHATZ, E. & AHLERS, G. 2012*a* Heat transport by turbulent Rayleigh–Bénard convection for $Pr \simeq 0.8$ and $4 \times 10^{11} \lesssim Ra \lesssim 2 \times 10^{14}$: ultimate-state transition for aspect ratio $\Gamma = 1.00$. *New J. Phys.* **14**, 063030.

HE, X., FUNFSCHILLING, D., NOBACH, H., BODENSCHATZ, E. & AHLERS, G. 2012*b* Transition to the ultimate state of turbulent Rayleigh–Bénard convection. *Phys. Rev. Lett.* **108**, 024502.

HE, X., FUNFSCHILLING, D., NOBACH, H., BODENSCHATZ, E. & AHLERS, G. 2013 Comment on 'Effect of boundary layers asymmetry on heat transfer efficiency in turbulent Rayleigh–Bénard convection at very high Rayleigh numbers'. *Phys. Rev. Lett.* **110**, 199401.

HE, X., VAN GILS, P. M., BODENSCHATZ, E. & AHLERS, G. 2014 Transition of heat transfer by turbulent Rayleigh–Bénard convection at high *Ra*. In *Abstract book of the EFMC 10 Conference, Copenhagen, Sept. 14–18*.

KRAICHNAN, R. H. 1962 Turbulent thermal convection at arbitrary Prandtl number. *Phys. Fluids* **5**, 1374–1389.

MALKUS, M. V. R. 1954 The heat transport and spectrum of thermal turbulence. *Proc. R. Soc. Lond.* A **225**, 196–212.

NIEMELA, J. J., SKRBEK, L., SREENIVASAN, K. R. & DONNELLY, R. J. 2000 Turbulent convection at very high Rayleigh numbers. *Nature* **404**, 837–840.

NIEMELA, J. J., SKRBEK, L., SREENIVASAN, K. R. & DONNELLY, R. J. 2001 The wind in confined thermal convection. *J. Fluid Mech.* **449**, 169–178.

NIEMELA, J. J. & SREENIVASAN, K. R. 2003 Confined turbulent convection. *J. Fluid Mech.* **481**, 355–384.

NIEMELA, J. J. & SREENIVASAN, K. R. 2006 The use of cryogenic helium for classical turbulence. *J. Low Temp. Phys.* **143**, 163–212.

NIEMELA, J. J. & SREENIVASAN, K. R. 2010 Does confined turbulent convection ever attain the 'asymptotic scaling' with 1/2-power? *New J. Phys.* **12**, 115002.

PRIESTLEY, C. H. B. 1959 *Turbulent Transfer in the Lower Atmosphere*. vol. 42, pp. 3650–3653. University of Chicago Press.

ROCHE, P. E., GAUTHIER, F., KAISER, R. & SALORT, J. 2010 On the triggering of the ultimate regime of convection. *New J. Phys.* **12**, 085014.

SHRAIMAN, B. I. & SIGGIA, E. D. 1990 Heat transport in high-Rayleigh number convection. *Phys. Rev.* A **42**, 3650–3653.

SPIEGEL, E. A. 1971 Convection in stars 1: basic Boussinesq convection. *Annu. Rev. Astron. Astrophys.* **9**, 323.

SREENIVASAN, K. R. 1998 Helium flows at ultra-high Reynolds and Rayleigh numbers. In *Flow at ultra-high Reynolds and Rayleigh numbers* (ed. R. J. Donnelly & K. R. Sreenivasan), pp. 29–51. Springer.

STEVENS, R. J. A. M., VAN DER POEL, E. P., GROSSMANN, S. & LOHSE, D. 2013 The unifying theory of scaling in thermal convection: the updated prefactors. *J. Fluid Mech.* **730**, 295–308.

THALABARD, S., SAINT-MICHEL, B., HERBERT, E., DAVIAUD, F. & DUBRULLE, B. 2015 A statistical mechanics framework for the large-scale structure of turbulent von Karman flows. *New J. Phys.* **17**, 063006.

TRITTON, D. J. 1988 *Physical Fluid Dynamics*. Oxford University Press.

URBAN, P., HANZELKA, P., KRÁLÍK, T., MUSILOVÁ, V., SKRBEK, L. & SRNKA, A. 2010 Helium cryostat for experimental study of natural turbulent convection. *Rev. Sci. Instrum.* **81**, 085103.

URBAN, P., HANZELKA, P., KRÁLÍK, T., MUSILOVÁ, V., SRNKA, A. & SKRBEK, L. 2012 Effect of boundary layers asymmetry on heat transfer efficiency in turbulent Rayleigh–Bénard convection at very high Rayleigh numbers. *Phys. Rev. Lett.* **109**, 154301.

URBAN, P., HANZELKA, P., KRÁLÍK, T., MUSILOVÁ, V., SRNKA, A. & SKRBEK, L. 2013 Reply to Comment on 'Effect of boundary layers asymmetry on heat transfer efficiency in turbulent Rayleigh–Bénard convection at very high Rayleigh numbers'. *Phys. Rev. Lett.* **110**, 199402.

URBAN, P., HANZELKA, P., MUSILOVÁ, V., KRÁLÍK, T., LA MANTIA, M., SRNKA, A. & SKRBEK, L. 2014 Heat transfer in cryogenic helium gas by turbulent Rayleigh–Bénard convection in a cylindrical cell of aspect ratio 1. *New J. Phys.* **16**, 053042.

URBAN, P., MUSILOVÁ, V. & SKRBEK, L. 2011 Efficiency of heat transfer in turbulent Rayleigh–Bénard convection. *Phys. Rev. Lett.* **107**, 014302.

WU, X.-Z. 1991 Along a road to developed turbulence: free thermal convection in low temperature helium gas. PhD thesis, University of Chicago, pp. 1–123.

WU, X.-Z. & LIBCHABER, A. 1991 Non-Boussinesq effects in free thermal convection. *Phys. Rev.* A **43**, 2833–2839.

ZHONG, J. Q., FUNFSCHILLING, D. & AHLERS, G. 2009 Enhanced heat transport by turbulent two-phase Rayleigh–Bénard convection. *Phys. Rev. Lett.* **102**, 124501.